Density and Viscosity of Normal Fluid in Dilute Solutions of He^3 in He^4†

J. G. Dash and R. Dean Taylor
Los Alamos Scientific Laboratory, University of California, Los Alamos, New Mexico
(Received February 14, 1957)

The torsion pendulum technique has been applied to the study of normal fluid density and viscosity of dilute solutions of He^3 in He^4 from 1.3°K to the lambda points. Three isotopic mixtures and pure He^4 have yielded data which cover the range from 0 to 11 mole percent He^3 concentration. Lambda temperatures are found to vary as the two-thirds power of the He^4 mole fraction. Densities at T_λ indicate a liquid volume contraction proportional to the concentration of He^3. Normal fluid densities at lower temperatures are described by a single analytic function for all solutions and temperatures studied. The experimental values may be interpreted in terms of an effective hydrodynamic density of He^3; empirical behavior of the effective He^3 density is seen to increase linearly with the density of superfluid, in qualitative agreement with the model suggested by Feynman. Viscosities of all solutions exhibit temperature variations similar to that of pure He^4. Dependence of the viscosity on He^3 concentration appears to be markedly nonlinear at all temperatures. Analysis of the data in terms of the Landau-Khalatnikov theory of viscosity, together with additional simple assumptions, yields an empirical estimate of the roton-He^3 atom collision cross section.

I. INTRODUCTION

THE addition of small amounts of He^3 produces marked changes in the properties of liquid He^4 below its lambda point. Although the dependence of some He II phenomena on He^3 concentration has been studied in detail, previous investigations have not included direct measurements of the normal fluid densities and viscosities, information necessary for a description of the hydrodynamics of the solutions below their lambda points. Direct measurement of normal fluid density and viscosity can be obtained by means of the torsion pendulum techniques used in studies[1,2] of the pure liquids He^3 and He^4. These papers, which will be referred to here as I and II, contain a description of the method and theoretical analysis.

We have studied He^3-He^4 solutions with the cryostat and torsion pendulum design described in II. This earlier report on the viscosities of liquid He^3 and of liquid He^4 above its lambda point was based upon the behavior of a single disk oscillating in the liquids. In the present work, observations of a single disk in He^3-He^4 solutions below T_λ were supplemented by studies of a finned rotor in the same solutions; the independent sets of data were combined as in I to yield the density and viscosity of the normal fluid component at temperatures from 1.28°K to the lambda point of He^4 and for He^3 concentrations from 0 to 10.8 mole percent.

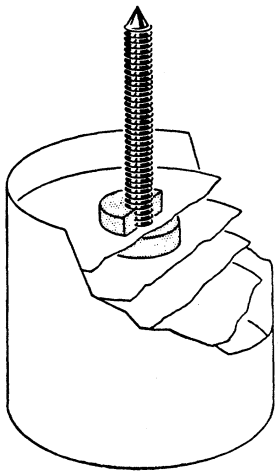

FIG. 1. Schematic drawing of Rotor (S) construction.

II. EXPERIMENTAL DETAILS

Cryostat construction is fully described in II. Chronograph and optical lever design and performance are given in I. The torsion pendulum and Disk (S) used here were identical to those used in II. Finned rotor studies were performed with a small Rotor (S) of a design similar to one described by Andronikashvili[3] and shown schematically in Fig. 1. Fifty thin aluminum disks were alternated with 50 spacers of smaller diameter within a thin Dural cylindrical shell. Dimensions of the Rotor (S) components are: aluminum disks, 0.617 cm radius, 0.0011 cm thick; Dural spacers, 0.238 cm radius, 0.019 cm thick; Dural cylinder, 1.262 cm o.d., 0.0038 cm wall thickness, 1.031 cm high. The Dural mandrel of the rotor was fitted with a small nut and was cemented to the lower end of the Pyrex tube of the pendulum. Dimensions and characteristics of the single Disk (S) pendulum are given in II.

Calibration Procedures

The period τ_0* of the Rotor (S) pendulum in vacuum at liquid helium temperatures was determined by a procedure similar to that described in I. Its period was measured as a function of He gas pressure while the cell was surrounded by a liquid helium bath. Rotor period varied linearly with gas pressure in the range

† A preliminary report on this research was presented at *The Third International Conference on Low Temperature Physics and Chemistry, December 17–22, 1953* (Rice Institute, Houston, 1953).

[1] J. G. Dash and R. D. Taylor, Phys. Rev. **105**, 7 (1957).

[2] R. D. Taylor and J. G. Dash, Phys. Rev. **106**, 398 (1957).

[3] E. L. Andronikashvili, J. Phys. (U.S.S.R.) **10**, 201 (1946).

from 500 to 1 mm Hg pressure, as shown in Fig. 2. Extrapolation yielded $\tau_0^*=5.2680$ sec.

Rotor characteristics required as constants in the equations of motion [Eqs. (30a, b) of I] are the spacer and cylinder radii, the cylinder height, spacing between disks, and total moment of inertia. Values for the radii and cylinder height were taken as the dimensions measured at room temperature and corrected by the total thermal contraction coefficient determined in I. Owing to the small size and complexity of Rotor (S), room temperature measurements of the moment of inertia and disk spacing were deemed unreliable; these constants were measured by calibration in liquid He^4. The equations of motion, together with known values of liquid density and viscosity, specify the experimental periods and decrements as functions of the disk spacing and moment of inertia. Using the values of ρ_n and η given in I, measurements of Rotor (S) behavior in pure He^4 near T_λ were thus made to yield the required parameters. In connection with Rotor ($L1$) in I, we discussed the effect of imperfections in the oscillations, such as are caused by warpage of the rotor disks. These imperfections cause an artificial increase in the measured value of ρ_n, the increase being proportional to the actual density of superfluid. Such distortions could be expected to be present in Rotor (S); we therefore determined their effect by comparison with the low-temperature results of Rotor ($L2$), where no imperfections in the oscillations were apparent. As a check on the parameters, iterations of the pure He^4 data given by Disk (S) and Rotor (S) were then carried out on an IBM 704 computer according to the calculation scheme to be used later in analyzing the solution data. Final values adopted for the calibrated quantities were: moment of inertia $I=0.09069$ g cm^2; spacing $2s=0.02040$ cm; superfluid excitation, 3.4%. The calculation scheme was not completely accurate, since the computing machine iterations were made with the Eq. (30a) for the rotor, which assumes no imperfections in the shear oscillations. Corrections for superfluid excitation was applied to the ρ_n and η results of the machine calculations. This procedure, which avoided considerably more complicated iterations, introduces second-order errors in the penetration depths; the resulting estimated uncertainties in final values of ρ_n and η are given in the section on experimental errors.

Percentage deviations of these new ρ_n values from the smoothed data of paper I is shown in Fig. 7; mean deviation is 1.83%.

Vapor pressure measurements taken during the pure He^4 studies showed that the cell liquid tended to be slightly warmer than the bath. This effect, presumably due to the "Kapitza resistance"[4] of the liquids, varied from zero at the lambda point to about 6 millidegrees at 1.3°K. Careful comparison of cell and bath temperatures yielded a calibration table of temperature difference as a function of He^4 bath temperature.

Solution Measurements

Three gaseous mixtures of pure He^3 and He^4 were prepared and stored in glass bulbs. The percentage He^3 molar concentrations were; sample A, 3.8%; B, 6.6%; C, 11%. Following the procedure used in II, samples were condensed in the cell via a mercury Toepler pump and liquid helium cooled impurity trap. He^4 bath temperature was stabilized to within 10^{-4} deg by an electronic bath regulator and throttled vacuum pump. Solution temperature was determined from the vapor pressure of the bath, the "1955E" vapor pressure scale,[5] and the calibration curve of temperature difference between the bath and cell. The relatively large vapor volume of the solution chamber caused appreciable fractionation of the solutions, and required the measurement of liquid concentration at each experimental point. The molar concentrations were therefore determined from the smooth table given by Sommers[6] and the measured vapor pressures and temperatures of the cell liquid.

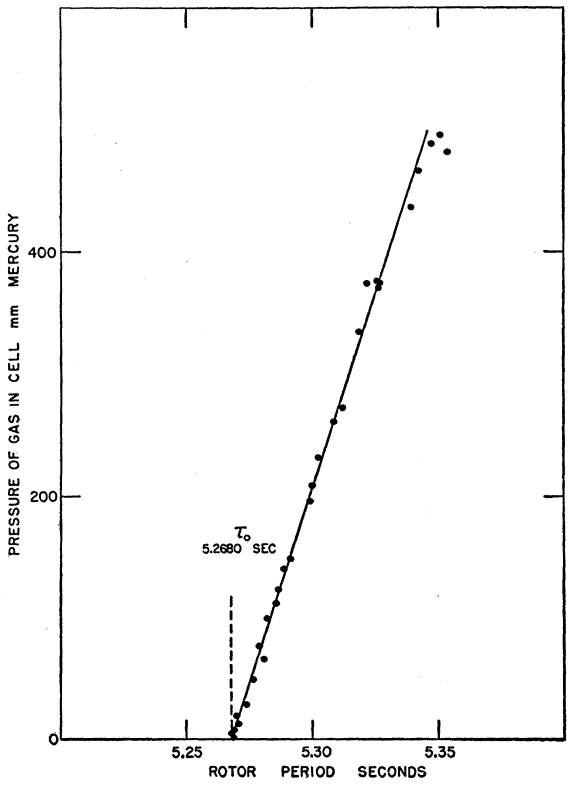

FIG. 2. Variation of rotor period with He gas pressure at 4°K.

[4] P. L. Kapitza, J. Phys. (U.S.S.R.) 4, 181 (1941).

[5] Clement, Logan, and Gaffney, Phys. Rev. **100**, 743 (1955); see their "Note added in proof;" W. E. Keller, Nature **178**, 883 (1956).

[6] H. S. Sommers, Jr., Phys. Rev. **88**, 113 (1952).

TABLE I. Experimental data.

T °K	Mole % He^3	τ^* sec	$10^3\delta$	τ sec	η micro-poise	ρ_n g/cm³
1.515	0.0	5.432	2.270	5.793	17.03	0.01610
1.600		5.477	2.455	5.794	15.77	0.02259
1.740		5.572	2.815	5.798	14.82	0.03676
1.853		5.665	3.185	5.802	15.15	0.05110
1.946		5.764	3.580	5.806	15.87	0.06690
2.024		5.868	4.005	5.810	16.91	0.08399
2.102		6.010	4.680	5.815	19.44	0.10725
2.166		6.198	5.820	5.822	25.35	0.13683
2.375		6.267	6.91	5.830	34.92	0.14397
2.299		6.260	6.74	5.830	33.24	0.14349
2.139		6.100	5.200	5.819	22.01	0.12150
2.058		5.926	4.255	5.812	17.67	0.09363
1.987		5.815	3.785	5.808	16.33	0.07523
1.885		5.698	3.310	5.804	15.28	0.05634
1.663		5.518	2.605	5.796	15.05	0.02865
1.419		5.391	2.065	5.790	19.02	0.01036
1.325		5.362	1.890	5.789	22.20	0.00641
1.351		5.368	1.935	5.789	21.49	0.00721
1.480		5.417	2.190	5.792	17.38	0.01400
1.657		5.513	2.590	5.796	15.17	0.02789
1.801		5.622	3.000	5.800	14.75	0.04446
2.037		5.890	4.095	5.811	17.14	0.08767
2.083		5.971	4.475	5.814	18.54	0.10097
2.121		6.054	4.920	5.817	20.55	0.11431
2.151		6.137	5.440	5.819	23.34	0.12720
2.1713		6.240	6.065	5.824	26.55	0.14365
2.1730		6.246	6.180	5.824	27.57	0.14403
2.248		6.256	6.58	5.830	31.59	0.14358
2.432		6.259	6.99	5.830	36.15	0.14214
2.169		6.214	5.950	5.823	26.20	0.13914
2.156		6.157	5.530	5.821	23.63	0.13063
1.802	3.08	5.6815	3.13	5.784	13.70	0.05449
1.893	3.22	5.7717	3.48	5.786	14.36	0.06922
2.047	3.50	5.9962	4.55	5.792	18.42	0.10574
2.106	3.50	6.1426	5.38	5.797	22.41	0.12909
2.124	3.7	6.2243	5.80	5.796	24.14	0.14280
2.171	3.7	6.2334	6.3	5.799	29.15	0.14094
2.137	3.7	6.2284	5.98	5.798	25.89	0.14214
2.119	3.70	6.2266	5.69	5.798	22.94	0.14434
2.116	3.60	6.2003	5.60	5.796	22.84	0.13948
2.086	3.64	6.0966	5.08	5.794	20.75	0.12206
2.001	3.50	5.9215	4.14	5.790	16.49	0.09393
1.704	3.21	5.6101	2.89	5.783	13.80	0.04302
1.506	3.45	5.4981	2.52	5.783	15.03	0.02585
1.311	3.63	5.4285	2.29	5.783	17.80	0.01564
1.277	3.81	5.4219	2.27	5.783	18.32	0.01469
1.410	3.40	5.4586	2.39	5.783	16.23	0.02001
1.609	3.25	5.5503	2.68	5.783	14.04	0.03377
1.952	3.50	5.8460	3.80	5.788	15.33	0.08143
1.826	5.43	5.7468	3.33	5.783	13.54	0.06556
1.886	5.42	5.8077	3.58	5.785	14.21	0.07564
1.990	5.64	5.9523	4.22	5.788	16.33	0.09978
2.086	5.67	6.2012	5.49	5.793	21.67	0.14092
2.134	6.0	6.2252	5.87	5.795	24.83	0.14238
1.904	5.75	5.8301	3.69	5.785	14.65	0.07923
1.517	6.55	5.5577	2.71	5.780	14.02	0.03494
1.408	6.64	5.5053	2.58	5.780	15.45	0.02687
1.318	6.69	5.4732	2.55	5.780	17.76	0.02194
1.804	5.40	5.7253	3.26	5.782	13.53	0.06191
1.900	5.88	5.8316	3.67	5.785	14.38	0.07974
1.999	5.77	5.9659	4.31	5.788	16.84	0.10175
2.047	5.85	6.0631	4.84	5.791	19.30	0.11728
2.080	5.85	6.1611	5.43	5.792	22.31	0.13266
2.103	6.0	6.2162	5.73	5.793	23.66	0.14175
2.165	6.1	6.2265	6.00	5.795	26.15	0.14161
2.191	6.1	6.2333	6.05	5.795	26.46	0.14261
2.093	6.0	6.2164	5.69	5.794	23.24	0.14216
2.062	5.95	6.1179	5.09	5.791	20.16	0.12668
2.028	5.95	6.0293	4.63	5.790	18.18	0.11214
1.962	5.92	5.9113	4.05	5.787	15.85	0.09274
1.753	5.88	5.6874	3.13	5.782	13.45	0.05563
1.659	5.68	5.6219	2.87	5.780	12.98	0.04523
1.556	5.78	5.5639	2.69	5.780	13.40	0.03604
1.461	6.01	5.5207	2.61	5.780	14.82	0.02924
1.318	6.22	5.4740	2.51	5.780	16.92	0.02216
2.048	6.06	6.0720	4.90	5.791	19.64	0.11860
1.901	9.23	5.9160	4.07	5.794	15.92	0.09358
1.982	9.15	6.0312	4.75	5.798	19.39	0.11136
2.008	9.20	6.0926	5.07	5.799	20.77	0.12140
2.151	9.3	6.1972	5.94	5.803	26.50	0.13620
2.037	9.3	6.1864	5.59	5.800	23.16	0.13676
2.027	9.25	6.1672	5.39	5.800	21.72	0.13443
2.014	9.30	6.1190	5.17	5.800	20.97	0.12612
2.000	9.25	6.0794	4.97	5.799	20.15	0.11953
1.960	9.35	5.9990	4.56	5.797	18.43	0.10634
1.848	9.25	5.8392	3.79	5.793	15.44	0.08024
1.752	9.58	5.7511	3.45	5.790	14.76	0.06556
1.659	10.00	5.6912	3.23	5.788	14.49	0.05579
1.557	10.15	5.6301	3.06	5.786	15.04	0.04584
1.457	10.46	5.5786	2.95	5.785	16.27	0.03763
1.364	10.38	5.5484	2.89	5.784	17.30	0.03293
1.286	10.81	5.5254	2.89	5.784	19.07	0.02930
1.903	9.45	5.9084	4.13	5.794	16.81	0.09139
2.095	9.3	6.2036	5.78	5.802	24.60	0.13867
2.057	9.3	6.2006	5.67	5.801	23.55	0.13900

Observations of pendulum behavior were made according to the schemes described in I and II. Rotor periods τ^* were obtained by averaging the times of at least 3 sets of 10 oscillations at each temperature; mean deviations of τ^* were within 2×10^{-3} sec. Disk decrements at every point were given by the average of two or more decay curves of at least 20 oscillations each; these individual decrements differed by less than 2%.

The Disk (S) data were interpolated in temperature and concentration in order to obtain Disk (S) data at temperatures and concentrations corresponding to the Rotor (S) points; calculations according to the established scheme yielded values of ρ_n and η for each Rotor (S) experimental point. Table I lists these input and derived data.

Discussion of Errors

The normalization of Rotor (S) characteristics in liquid He^4 cause the new results to be subject to the uncertainties in the smoothed I data. For normal densities, these are 0.9% at T_λ and 3.4% at 1.3°K. The Rotor (S) periods were reliable to better than 5×10^{-3} sec all temperatures, implying a ρ_n uncertainty within 0.5% at T_λ and 3% at 1.3°K. The incompleteness of the calculating scheme, due to the neglect of the influence of superfluid excitation on the calculated penetration depth, introduces estimated errors which vary from zero at T_λ to 4% at the lowest temperatures. Thus, the maximum combined uncertainty in ρ_n due to the above causes is approximately 1.5% at T_λ and 10% at 1.3°K.

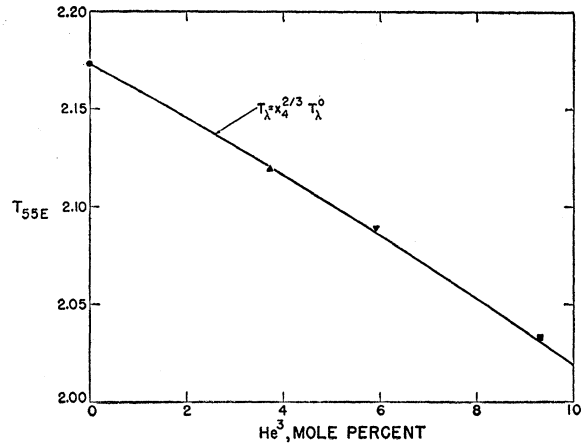

FIG. 3. Variation of lambda temperature with He^3 concentration.

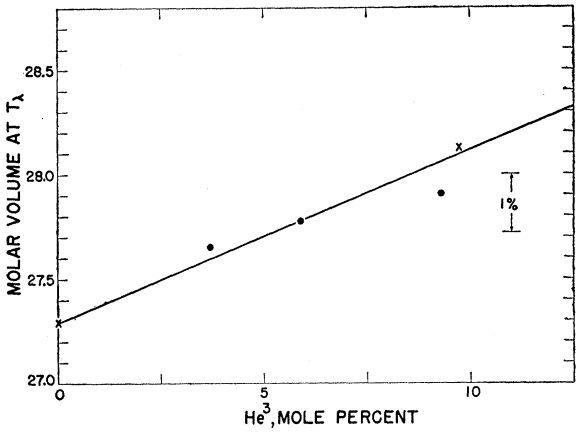

FIG. 4. Dependence of molar volume of solution at T_λ on He^3 concentration. ● this research; × pycnometric measurements of Kerr.[9,11]

Similarly, the estimated uncertainty in η is 5% at high temperatures and 20% at 1.3°K.

We estimate the reliability of temperature measurement as better than 10^{-3} deg at high temperatures and 3×10^{-3} deg in the lower range.

Uncertainties in temperature and vapor pressure of the solutions lead to errors in the computed He^3 concentrations. These errors are estimated to be within 5% of the measured values of x_3 at all temperatures.

III. NORMAL FLUID DENSITY

Analysis of the data requires repeated reference to certain liquid properties whose algebraic symbols and definitions have not been standardized. With an attempt to maintain general usage wherever it exists, we define the quantities and notation to be used here. As denoted by most previous authors, we label properties of the individual isotopes by subscripts 3 or 4; in the case of the pure isotopes we add the superscript 0. For some characteristics of pure He^4 below its lambda point, we may omit the subscript without incurring confusion.

N_3^0: number density of atoms in pure He^3,
N_3: number density of He^3 atoms in solution,
ρ_3^0: mass density of pure He^3,
ρ_3: effective mass density of He^3 in solution, M_3/V_3,
V_3^0: molar volume of pure He^3,
V_3: partial molar volume of He^3 in solution,
T_λ: lambda-point temperature of solution,
$T_{4\lambda}^0=T_\lambda^0$: lambda-point temperature of pure He^4,
ρ: mass density of solution,
ρ_λ: mass density of solution at T_λ,
$\rho_{4\lambda}^0=\rho_\lambda^0$: mass density of pure He^4 at T_λ^0,
x_3: mole fraction of He^3, $N_3/(N_3+N_4)$,
φ_3: volume fraction of He^3,
w_3: weight fraction of He^3,
T^*: reduced temperature, T/T_λ,
ρ_3^*: effective hydrodynamic density of He^3 in solution.

Lambda-Point Temperatures and Densities

Large graphs of normal density plotted *versus* temperature indicate the coordinates ρ_λ and T_λ of the lambda point of each sample. The experimental values of T_λ are shown in Fig. 3. As in the case of T_λ determined from the 1948 temperature scale,[7] the present results given in terms of the "1955*E*" scale are within 2×10^{-3} deg of the semiempirical function,[8]

$$T_\lambda = x_4^{\frac{3}{4}} T_\lambda^0, \tag{1}$$

where now $T_\lambda^0=2.1735$°K.

The variation of molar volume,

$$V_\lambda = (3x_3+4x_4)/\rho_\lambda = x_3V_3+x_4V_4,$$

with x_3 is shown in Fig. 4. Our data are in agreement with the pycnometer results of Kerr[9] and show an appreciable volume contraction on mixing. The straight line drawn in Fig. 4, which describes the pycnometric measurements of ρ_λ to within 0.15% up to $x_3=0.50$, corresponds to

$$V_\lambda \text{ cm}^3/\text{mole} = 35.552x_3+27.291x_4.$$

The partial molar volume V_3 is approximately 8% smaller than that of the pure liquid at the same temperature; V_3^0 (2.0°K) = 38.456 cm³/mole.[10] The partial molar volume of He^4 corresponds to that of the pure liquid He^4 at T_λ^0.[11] As a more convenient property, we obtain an expression for the solution densities at T_λ

[7] J. G. Dash and R. D. Taylor, Phys. Rev. **99**, 598 (1955)
[8] L. Goldstein, Phys. Rev. **95**, 869 (1954).
[9] E. C. Kerr (to be published). We thank Dr. Kerr for permission to quote his results in advance of publication.
[10] E. C. Kerr, Phys. Rev. **96**, 551 (1954).
[11] E. C. Kerr, J. Chem. Phys. **26**, 511 (1957).

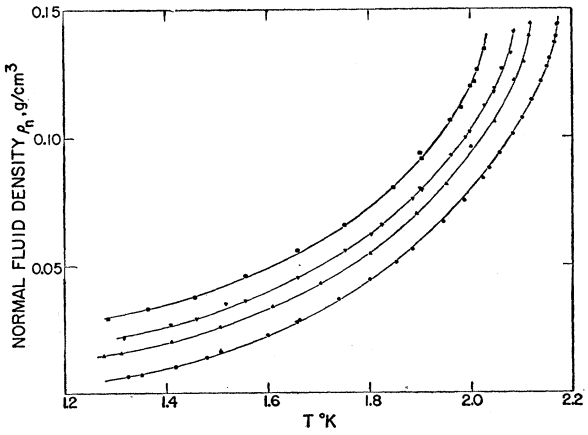

FIG. 5. Normal fluid densities of He^3-He^4 solutions. ● pure He^4; ▲ sample A; ▼ sample B; ■ sample C.

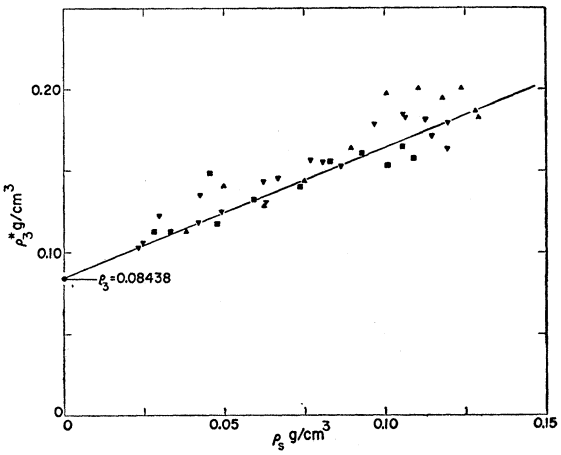

FIG. 6. Effective hydrodynamic density of He^3 in solution *versus* density of superfluid. ● mean value at T_λ; ▲ sample A; ▼ sample B; ■ sample C.

derived from the empirical molar volumes[12]:

$$\begin{aligned}&\rho_\lambda=\varphi_4\rho_\lambda{}^0+\varphi_3\rho_3;\\&\rho_3=0.08438\ \text{g/cm}^3,\quad \rho_\lambda{}^0=0.014657\ \text{g/cm}^3,\\&\varphi_3=\frac{x_3V_3}{V_\lambda}=x_3\left[x_3+x_4\left(\frac{m_4\rho_3}{m_3\rho_4}\right)\right]^{-1},\quad \varphi_4=1-\varphi_3.\end{aligned}\tag{2}$$

The change in total density due to thermal contraction below T_λ for concentrations $0\leq x_3\leq 0.10$ is not greater than 0.8% of ρ_λ;[9] in the following analysis we shall therefore approximate $\rho(T\leq T_\lambda)=\rho_\lambda$ and compute ρ from Eq. (2).

Analysis of ρ_n Data

Values of ρ_n listed in Table I are shown graphically *versus* temperature in Fig. 5. The smooth curves drawn through experimental points do not represent lines of constant concentration, but only serve to connect the data corresponding to each sample A, B, C. Within the concentration range of each sample, the curves show qualitative features which have helped in the choice of methods for analyzing the data.

The lateral shifts in the curves caused by the lambda-point depressions suggest that the various solutions should be compared at corresponding "stages of degeneration" below their individual values of T_λ. Such a comparison can be approximated by means of the "reduced temperature" $T^*=T/T_\lambda$.[13] When considering their superfluid properties, it is obvious that mixtures of differing concentrations are equivalent at $T^*=1$; we shall assume that the correspondence holds for all values of T^*. Thus, solutions of different molar concentrations x_i, x_j are considered to be at corresponding temperatures T_i, T_j when they are at the same reduced temperature referred to their individual lambda points:

$$T^*=\frac{T_i}{T_\lambda(x_i)}=\frac{T_j}{T_\lambda(x_j)}.\tag{3}$$

When one examines the experimental results in terms of T^*, each sample curve appears to approach an asymptotic value of ρ_n at low T^*; the asymptotic values increase with increasing x_3. This behavior is in qualitative agreement with the prediction[14] that the He^3 atoms move with the normal fluid. Superposition of contributions of the He^4 and He^3 components to ρ_n has been assumed by Pomeranchuk[15]:

$$\rho_n=\rho_{4n}+N_3\mu_3,$$

where ρ_{4n} is the contribution due to the He^4, N_3 is the number of He^3 atoms per unit volume, and μ_3 is the effective mass of the He^3 atoms. Although we shall assume linear superposition of the He^3 and He^4 contributions, the above formula is not satisfactory for quantitative comparison with the data.[16] We shall assume an equation for superposition based upon the correspondence of reduced temperatures and which satisfies Eq. (2) at $T^*=1$:

$$\rho_n(T^*,\varphi_3)=\varphi_4\rho_n(T^*,\ \varphi_3=0)+\varphi_3\rho_3{}^*.\tag{4}$$

[12] For ideal solutions, the linear superposition of component densities according to the mass concentration, as implied by P. J. Price, reference 16, and F. London, *Superfluids* (John Wiley and Sons, Inc., New York, 1954), Vol. 2, p. 195, is not appropriate. For dilute He^3-He^4 solutions, $w_3\simeq 0.75x_3\simeq 0.58\varphi_3$; improper specification of the concentration may in some cases lead to corresponding errors in deduced quantities.

[13] The reduced temperature ratio has previously been employed in similar fashion by L. Goldstein, reference 8.

[14] E. Pollard and W. L. Davidson, *Applied Nuclear Physics* (John Wiley and Sons, Inc., New York, 1942), p. 183; J. Franck, Phys. Rev. **70**, 561 (1946); L. Landau and I. Pomeranchuk, Doklady Acad. Nauk (U.S.S.R.) **59**, 669 (1948).

[15] I. Pomeranchuk, J. Exptl. Theoret. Phys. (U.S.S.R.) **19**, 42 (1949).

[16] P. J. Price, Phys. Rev. **89**, 1209 (1953). Price has remarked on the failure of Pomeranchuk's formula to describe the solution densities correctly at $T=T_\lambda$.

TABLE II. Normal fluid densities in g/cm³ at regular intervals of reduced temperature and He³ mole fraction.

T^* \ x_3	0	0.01	0.02	0.03	0.04	0.05	0.06	0.07	0.08	0.09	0.10	0.11
1.000	0.14657	0.14576	0.14496	0.14416	0.14337	0.14258	0.14180	0.14102	0.14024	0.13947	0.13871	0.13795
0.995	0.13371	0.13320	0.13269	0.13217	0.13165	0.13113	0.13061	0.13008	0.12956	0.12903	0.12850	0.12797
0.990	0.12776	0.12739	0.12701	0.12662	0.12623	0.12583	0.12543	0.12502	0.12461	0.12420	0.12378	0.12335
0.985	0.12261	0.12236	0.12209	0.12182	0.12154	0.12125	0.12095	0.12064	0.12033	0.12001	0.11969	0.11936
0.980	0.11781	0.11767	0.11751	0.11734	0.11716	0.11697	0.11677	0.11656	0.11634	0.11612	0.11588	0.11564
0.975	0.11354	0.11349	0.11344	0.11336	0.11327	0.11317	0.11306	0.11293	0.11280	0.11265	0.11249	0.11232
0.970	0.10959	0.10964	0.10967	0.10968	0.10967	0.10965	0.10962	0.10957	0.10951	0.10944	0.10936	0.10926
0.965	0.10587	0.10600	0.10612	0.10621	0.10628	0.10634	0.10638	0.10641	0.10642	0.10642	0.10640	0.10637
0.960	0.10242	0.10263	0.10282	0.10299	0.10314	0.10327	0.10338	0.10348	0.10356	0.10362	0.10367	0.10370
0.955	0.09916	0.09945	0.09971	0.09995	0.10017	0.10037	0.10055	0.10071	0.10085	0.10097	0.10108	0.10117
0.950	0.09608	0.09644	0.09677	0.09708	0.09736	0.09763	0.09787	0.09809	0.09829	0.09847	0.09863	0.09878
0.945	0.09310	0.09353	0.09393	0.09430	0.09465	0.09497	0.09527	0.09555	0.09581	0.09605	0.09627	0.09647
0.940	0.09017	0.09065	0.09112	0.09156	0.09197	0.09235	0.09272	0.09305	0.09337	0.09366	0.09394	0.09419
0.935	0.08735	0.08791	0.08844	0.08894	0.08941	0.08985	0.09027	0.09066	0.09103	0.09138	0.09171	0.09201
0.930	0.08459	0.08521	0.08581	0.08636	0.08689	0.08740	0.08787	0.08832	0.08874	0.08914	0.08952	0.08987
0.925	0.08195	0.08263	0.08329	0.08390	0.08449	0.08504	0.08557	0.08607	0.08655	0.08700	0.08742	0.08782
0.920	0.07935	0.08009	0.08080	0.08148	0.08212	0.08273	0.08331	0.08386	0.08439	0.08488	0.08536	0.08580
0.900	0.07036	0.07131	0.07222	0.07309	0.07393	0.07473	0.07549	0.07622	0.07692	0.07758	0.07822	0.07883
0.880	0.06187	0.06302	0.06412	0.06518	0.06619	0.06717	0.06810	0.06900	0.06986	0.07069	0.07148	0.07224
0.860	0.05451	0.05583	0.05710	0.05831	0.05949	0.06061	0.06170	0.06274	0.06375	0.06471	0.06564	0.06654
0.840	0.04782	0.04929	0.05071	0.05208	0.05339	0.05466	0.05588	0.05705	0.05819	0.05928	0.06033	0.06135
0.820	0.04163	0.04324	0.04480	0.04630	0.04775	0.04915	0.05049	0.05179	0.05304	0.05425	0.05542	0.05654
0.800	0.03623	0.03797	0.03965	0.04127	0.04283	0.04434	0.04579	0.04720	0.04856	0.04987	0.05113	0.05236
0.780	0.03152	0.03337	0.03515	0.03688	0.03854	0.04014	0.04170	0.04319	0.04464	0.04604	0.04740	0.04870
0.760	0.02707	0.02902	0.03091	0.03273	0.03448	0.03618	0.03782	0.03941	0.04094	0.04243	0.04386	0.04525
0.740	0.02325	0.02529	0.02726	0.02916	0.03100	0.03278	0.03450	0.03616	0.03777	0.03933	0.04083	0.04229
0.720	0.01973	0.02185	0.02390	0.02588	0.02780	0.02965	0.03144	0.03317	0.03485	0.03647	0.03804	0.03956
0.700	0.01658	0.01877	0.02089	0.02294	0.02493	0.02684	0.02870	0.03049	0.03223	0.03391	0.03554	0.03711
0.680	0.01375	0.01601	0.01819	0.02030	0.02235	0.02432	0.02623	0.02808	0.02988	0.03161	0.03329	0.03492
0.660	0.01130	0.01362	0.01586	0.01802	0.02011	0.02214	0.02410	0.02600	0.02784	0.02962	0.03135	0.03302
0.640	0.00921	0.01157	0.01386	0.01607	0.01821	0.02028	0.02228	0.02422	0.02610	0.02792	0.02969	0.03140
0.620	0.00737	0.00978	0.01210	0.01435	0.01653	0.01864	0.02068	0.02266	0.02457	0.02643	0.02823	0.02997
0.600	0.00576	0.00820	0.01057	0.01285	0.01507	0.01721	0.01928	0.02129	0.02324	0.02512	0.02695	0.02872

Approximate correspondence between Eq. (4) and Pomeranchuk's formula at low values of φ_3 is obtained by setting the effective hydrodynamic He³ density $\rho_3^* = \mu_3\rho_3/m_3$; μ_3/m_3 must be unity at $T^*=1$.

The use of Eqs. (1)–(4) and $\rho_n(T^*, \varphi_3=0)$ from the smoothed data of I allows us to calculate ρ_3^* for each experimental ρ_n in Table I. These calculated ρ_3^* show definite regularities in their dependence on temperature and He³ concentration. Except for the region $0.97<T^*<1$, ρ_3^* increases with decreasing T^*, but tends rapidly toward asymptotic limits at low T^*. The limiting values of $\rho_3^*(\varphi_3, T^*<0.7)$ increase with decreasing He³ concentration. Within experimental uncertainty all values of ρ_3^* are described by the same linear function of the density of superfluid. Using the ρ_s calculated from the experimental data,

$$\rho_s(T^*,\varphi_3)=\rho_\lambda(\varphi_3)-\rho_n(T^*,\varphi_3), \tag{5}$$

we plot ρ_3^* *versus* density of superfluid in Fig. 6. The straight line average of the data, as shown in Fig. 6, corresponds to the equation

$$\rho_3^*=\rho_3+0.796\rho_s. \tag{6}$$

With Eqs. (1)–(6) we obtain a completely analytic expression for ρ_n (in terms of ρ_n of pure He⁴) for the temperature and concentration ranges studied:

$$\rho_n(T^*,\varphi_3)=\varphi_3\rho_3 + \left(\frac{\varphi_4}{1+\gamma\varphi_3}\right)[\rho_n(T^*, \varphi_3=0)+\gamma\varphi_3\rho_\lambda{}^0], \tag{7}$$

$$\rho_3=0.08438, \quad \rho_\lambda{}^0=0.14657, \quad \gamma=0.796.$$

It is noteworthy that the analysis depends on directly measured data only, except that the $\rho_n(T^*, \varphi_3=0)$ values from I have been smoothed. For convenience, we have used Eq. (7) to construct Table II, which lists values of ρ_n at regular intervals of T^* and x_3. The intervals are sufficiently small to permit linear interpolation in both directions. Deviations of the original ρ_n data from corresponding values according to Table II are shown in Fig. 7; mean percentage deviation in ρ_n for all points is 1.77%.

Discussion of ρ_n Results

Pellam[17] has studied the normal fluid density and viscosity of a solution containing 0.044 mole fraction of He³. These measurements, obtained from observations of the period and damping of a finned rotor, indi-

[17] J. R. Pellam, Phys. Rev. **99**, 1327 (1955).

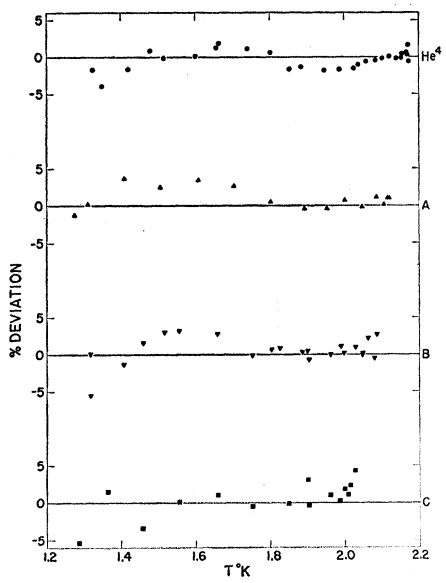

FIG. 7. Deviations of experimental normal fluid density data from values derived from Table II.

cate an asymptotic value of ρ_n/ρ at low temperatures which appears to be in qualitative agreement with our data.

For comparison with recent ρ_n measurements, see note added in proof.*

Experiments on the variation of second sound velocity with He^3 concentration have provided another, but less direct, method for deducing the He^3 effective mass. Such measurements,[18,19] analyzed by means of the dilute solution theory of Pomeranchuk,[15] have given values for μ_3 in qualitative disagreement with the findings reported here. The published μ_3 furthermore violate the requirement $\mu_3 \rightarrow m_3$ as $T \rightarrow T_\lambda$. There are, however, certain equivocal aspects of the second sound analysis; we shall suggest several modifications which yield calculated μ_3 values considerably different from those originally published.

The equation for second sound velocity u_2 in very dilute He^3-He^4 solutions, as derived by Pomeranchuk, is

$$u_2^2=\frac{T\rho_s}{\rho_n}\left[\left(S_4+\frac{k\epsilon}{m_4}\right)^2 C^{-1}+\frac{k\epsilon}{m_4}\right],$$

where S_4 is the entropy/gram of pure He^4, k is the Boltzmann constant, m_4 is the mass of the He^4 atom, C is the heat capacity/gram of solution, and ϵ is the "mole ratio" N_3/N_4. The specific heat of the dissolved He^3 is assumed to correspond to an ideal gas,[20]

$$C=C_4+\tfrac{3}{2}k\epsilon/m_4.$$

Accordingly, measurement of $u_2(\epsilon,T)$, together with known values[21] of the specific heat and entropy of pure He^4 suffice for the determination of $\rho_n(\epsilon,T)$. These values for the normal fluid density are then compared with the values for ρ_n calculated from second sound measurements in pure He^4; the change in ρ_n is ascribed to the He^3.

The application of these approximations to solutions of appreciable He^3 concentration requires somewhat more detailed treatment than that indicated by Pomeranchuk. Where properties of the solutions are assumed to be resultants of the linear superposition of the pure components, some account should be made of the reduction in the atomic density of the He^4; as in the case of ρ_n, Pomeranchuk has consistently neglected this effect. Although not explicit, the theory also apparently ignores the effect of the lambda-point depressions, implying that the contribution of the He^4 in a solution at some temperature corresponds to the value of the property in pure He^4 at the same temperature. It is unlikely that the published calculations of μ_3 could have taken into account the recently observed deviations from ideality of the total densities of the mixtures. We therefore recompute the He^3 effective mass from the published values for u_2, S_4, C_4 according to the same ideas on linear superposition and reduced temperature that formed the basis for analysis of our own data. Thus, we use Eqs. (1)–(5) of this paper, together with modified formulas for u_2 and C;

$$[u_2(T^*,\epsilon)]^2=T\frac{\rho_s}{\rho_n}(T^*,\epsilon)\times\left\{\left[w_4S(T^*,\epsilon=0)+\frac{k\epsilon}{m_4}\right]^2[C(T^*,\epsilon)]^{-1}+\frac{k\epsilon}{m_4}\right\},$$

$$C(T^*,\epsilon)=w_4C(T^*,\epsilon=0)+\tfrac{3}{2}k\epsilon/m_4.$$

Using these modified equations, we show in Fig. 8 the calculated ρ_3^* for a mixture of $x_3=0.008$; the new values are compared with the curve originally published[19] and with the trend corresponding to Eq. (6). The behavior of ρ_3^* as obtained from second sound studies is now in better agreement with the values obtained from the torsion pendulum data. In spite of these changes, the ρ_3^* calculated for higher concentrations and lower

* *Note added in proof.*—Brief description of ρ_n measurements in He^3—He^4 solutions by means of a torsion pendulum is given by N. G. Berezniak and B. N. Eselson, J. Exptl. Theoret. Phys. (U.S.S.R.) **31**, 902 (1956); Soviet Phys. 4, 766 (1957) (translation). Their results, for $x_3=0.0$, 0.03, 0.056, 0.082, and 1.4°K $<T<T_\lambda$, are in qualitative agreement with our findings. Discrepancies amounting to as much as 18% can be explained in their calculation of ρ_n/ρ to a first approximation only, apparently no account being made of variations in boundary layer thickness or of slippage of liquid between the disks. Their analysis for μ_3 was based upon the asymptotic formula of Pomeranchuk for very small x_3; deduced values for μ_3 therefore show an erroneous increase to very high values near T_λ.

[18] E. A. Lynton and H. A. Fairbank, Phys. Rev. **80**, 1043 (1950).

[19] J. C. King and H. A. Fairbank, Phys. Rev. **93**, 21 (1954).

[20] We are here considering the special case, in Pomeranchuk's treatment, of approximately zero minimum value for the dissolved He^3 momentum spectrum. According to his theory, this condition is indicated by the qualitative behavior of the ρ_n data and by the second sound velocity at very low temperatures.

[21] Kramers, Wasscher, and Gorter, Physica **18**, 329 (1952).

temperatures still show a positive temperature coefficient. These residual discrepancies may arise from the nature of the approximations in the Pomeranchuk's theory. It is also possible that the disagreement originates in the same sources that cause the unresolved discrepancies between the second sound and torsion pendulum values for ρ_n in pure He^4 (see I).

A division of normal density values into the separate contributions of the He^4 and He^3 as in the preceding analysis is an arbitrary procedure, since the torsion pendulum technique cannot distinguish between the isotopes excited by the oscillations of the rotor. Equation (4) is therefore only an assumption in the present treatment, although it is based upon theoretical considerations. Nevertheless, the use of the empirical relationship Eq. (6) and the final Eq. (7) yields values for ρ_n which may be considered as completely empirical in describing the original data. Agreement between Eq. (7) and the measurements is well within experimental accuracy throughout the range of study, except for $x_3>0.03$ at temperatures within 0.05°K of T_λ. The calculated ρ_n appear to lie systematically below the data in this narrow interval, indicating that the temperature dependence of ρ_n near T_λ becomes progressively less steep with increasing x_3. This effect is not very pronounced, however, since deviations of sample C points from the calculated values are no greater than 4.2%, less than 3 times the estimated accuracy at these temperatures.

If one accepts the theoretical implications of Eq. (4), the empirical values of ρ_3^* are in qualitative agreement with the behavior postulated by Feynman.[22] In this theoretical treatment, the He^3 atoms are considered to be analogous to small solid spheres moving through an ideal fluid. The solution of this familiar problem in classical hydrodynamics shows that the effective mass of the sphere is the sum of its "true" mass and one-half of the mass of displaced fluid. For He^3 atoms in very dilute solutions at $T=0$, the effective mass becomes

$$\mu_3=m_3+\tfrac{1}{2}(v_3/v_4)m_4,$$

where v_3, v_4 are the atomic volumes of the isotopes in the liquid. Substituting the value of v_3 corresponding to the pure liquid molar volume $V_3^0=38.46$ cm³ yields $\mu_3=5.82$ atomic mass units, as given by Feynman; use of the empirical volume in solution $V_3=35.55$ cm³ yields $\mu_3=5.61$ amu. In order to obtain the effective hydrodynamic density ρ_3^* for the He^3, the above formula is transformed by dividing through by v_3;

$$\rho_3^*=\rho_3+\tfrac{1}{2}\rho_4.$$

These expressions cannot be valid except where $T\simeq 0$, $x_3\simeq 0$. At higher temperatures and concentrations we may no longer consider each He^3 atom to be surrounded by superfluid He^4. Since it is only by *relative* motion

[22] R. P. Feynman, Phys. Rev. 94, 262 (1954).

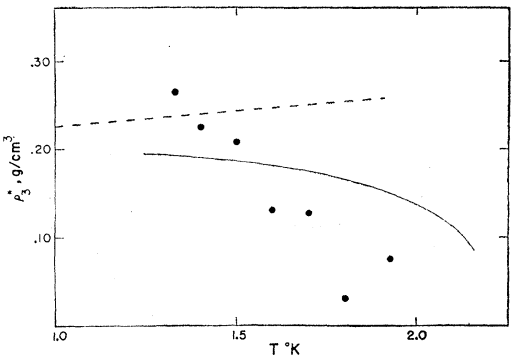

FIG. 8. Effective hydrodynamic density of He^3 in solution derived from second sound measurements. – – – behavior given by King and Fairbank[19]; ● calculated from data of King and Fairbank by means of modified formulas of Pomeranchuk; —— our results, Eq. (6).

that the mass (or density) of the He^3 is increased, the density of the fluid through which the He^3 moves is ρ_s. The theoretical effective hydrodynamic density at all T, x_3 is therefore

$$\rho_3^*=\rho_3+\tfrac{1}{2}\rho_s. \tag{8}$$

Equation (8) is formally identical with the Eq. (6). The empirical $\gamma=0.796$ appears to indicate only quantitative failure of classical hydrodynamics when applied to atomic dimensions. The discrepancy is perhaps understandable in terms of the details of the classical problem, for we might expect that the motion of a He^3 atom should create a disturbance of greater extent among the surrounding atoms than if the velocity gradients could decrease in a microscopically smooth and continuous fashion.

Alternatives to Eq. (4) could attribute some of the increase in normal fluid density to the He^4 component. The introduction of He^3 atoms into the He^4 is evidently a strong perturbation on the He II phase, as manifested by the lambda-point depression. The readjustment of the ρ_n behavior by means of reduced temperatures has made different solutions artificially equivalent at T_λ, but also tends to obscure one of the important phenomena. A more satisfactory view of the solutions might treat the increase in normal density as some kind of a composite of the He^3 and of a He^4 contribution enhanced by the presence of the He^3. Although we have not attempted to treat the experimental data according to this type of model, it is apparent that our results can be made to correspond to such a nonlinear alternative to Eq. (4).

IV. VISCOSITY

The measured viscosities of the solutions and of pure He^3 and He^4 are listed in Table I and are shown in Fig. 9. Here, as before, the smooth curves in Fig. 9 connect data points of each mixture and are not lines of constant concentration. All samples have the same

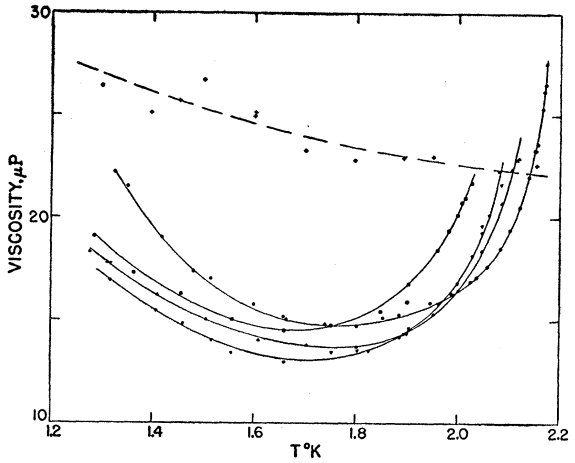

FIG. 9. Variation of viscosity of He^3-He^4 solutions with temperature. + pure He^3; ● pure He^4; ▲ sample A; ▼ sample B; ■ sample C.

qualitative behavior: an initially steep decline from the value at the lambda point, to a broad minimum at 1.6–1.8°K, followed by a continuous rise in η at lower temperatures. Comparison between the curves shows several interesting features.

(1) The lambda-point viscosity $\eta(T_\lambda,x_3)$ decreases with increasing x_3.

(2) The temperatures at which the viscosity reaches a minimum decrease with increasing x_3.

(3) The value of η at the minimum is initially depressed by the presence of He^3 for the more dilute solutions, but thereafter appears to increase with increasing He^3 concentration.

(4) The monotonic rise in η at low temperatures is less pronounced in the solutions.

At no temperature can the viscosity of the solutions be expressed as the linear superposition of the viscosities of the pure components. The nonlinear influence of the lighter isotope is clearly shown in Fig. 10(A), where we have plotted $\eta(T_\lambda,x_3)$ *versus* x_3. Values for the solutions appear to approach rapidly the viscosity of pure He^3 in the same temperature range. For solutions of higher concentration, $\eta(T_\lambda,x_3)$ probably eventually rises again, in order to approach the increased viscosity of He^3 at lower temperatures. The dependence of η on x_3 at the minimum appears to follow a more complicated dependence on x_3. As shown in Fig. 10(B), the curve of η (minimum) *versus* x_3 seems to have a minimum of its own at $x_3 \sim 5\%$. The viscosity at these temperatures cannot be described by any form of superposition, since the viscosity of the solutions becomes less than the viscosity of either pure component. Although the decreasing dependability of the data makes generalizations hazardous at lower temperatures, the qualitative variation of η with x_3 in Fig. 10(B) is apparently maintained down to 1.3°K.

Discussion of Viscosity Results

Our viscosity results are in strong disagreement with the measurements of Pellam,[17] who reports a monotonic decrease in η with temperature, approximately proportional to ρ_n; his estimated value for the viscosity at 1°K is 4–5 micropoise. The calculation apparently involved a normalization at T_λ, although the details of the calculation are not given. We believe that this discrepancy can be attributed in large part to the difference in temperature dependences of the corrections due to the "internal friction" (see I) and boundary layer of the rotor.

No theory has yet successfully described the viscosity of pure He^4 over the entire range of temperatures covered in the present study. Landau and Khalatnikov[23] have calculated the viscosity at temperatures below the viscosity minimum on the basis of the quantum-hydrodynamical model, but have not succeeded in applying these ideas to the warmer region of high roton density. Although a more complete theoretical description of pure He^4 must probably precede a clear understanding of He^3-He^4 solutions, the empirical behavior of the mixtures suggests theoretical implications which we shall report here.

The apparent correspondence between the ρ_n contribution of the dissolved He^3 and the sphere problem of classical hydrodynamics implies that the analogy might describe the viscosity effects equally well. Einstein[24] has calculated the influence of a dilute concentration of small neutral spheres suspended in a liquid; the viscosity is shown to be increased as $\frac{5}{2}$ times the volume concentration of the suspended particles. This result, yielding an effect of opposite sign to that of the He solutions, is apparently restricted to the case of particles considerably larger than the atoms of the liquid. A more promising domain to consider might be the behavior of gaseous mixtures, as treated by Chapman.[25] The addition of chemically inert atoms to a gas of heavier atoms is found generally to increase the viscosity of the mixture above the value given by linear superposition. This tendency, again opposite to the behavior of the He solutions, may be understood as the resultant of three factors; a reduction of the mean free path of the heavier atoms, an increase in the number of momentum carriers, and a tendency toward persistence of the heavy atoms' initial momenta after collision with the lighter particles. The first two factors cancel to a first approximation, leaving the third as a dominant tendency toward an increase in the viscosity. The tendency toward a viscosity increase may also be

[23] L. D. Landau and I. M. Khalatnikov, J. Exptl. Theoret. Phys. (U.S.S.R.) **19**, 637, 709 (1949).

[24] A. Einstein, Ann. Physik **19**, 289 (1906); **34**, 591 (1911): also in collected papers, *Theory of the Brownian Movement*, edited by R. Fürth and A. D. Cowper (Dover Publications, New York, 1956).

[25] S. Chapman and T. G. Cowling, *The Mathematical Theory of Nonuniform Gases* (Cambridge University Press, New York, 1953).

considered as the result of a decreased average collision cross section.

It appears that an explanation for the decreased viscosity of He^3-He^4 solutions must be sought in the unusual character of the He II energy spectrum. According to the work of Landau and Khalatnikov,[23] the viscosity of He II above 0.8°K results from the scattering of phonons and rotons by rotons; above about 1.5°K, roton-roton scattering is dominant. We shall assume that He II in the high-temperature region can indeed be treated as a roton gas. These excitations may be treated as elementary vortices of 7 or so He^4 atoms, and whose internal energy is quantized. An encounter between such a He^4 vortex and a He^3 atom must evidently produce a strong perturbation on the roton, for it may not drift through the region of the He^3 atom without a change in its quantized internal energy. We therefore expect a high probability for a deflection of the original drift direction of the roton. Hence, the presence of the He^3 decreases the roton mean free path. If there is any He^3-induced decrease in the density of the rotons, the effect on the viscosity should be compensated by a corresponding increase in the roton-roton collision free path. The He^3 atoms themselves, if sufficiently dilute, will not contribute a significant increase in momentum transport. The net effect of the He^3 is a decrease in the viscosity.

Since the viscosity of He II at the minimum is almost completely due to rotons, we can make a crude numerical test of these speculations. We find that η (minimum) is decreased from 14.7 micropoise in pure He^4 to 13.7 micropoise when $x_3=0.031$, or $N_3=6.8\times10^{20}$ atoms/cm^3. Using the relation[26] $\rho_n/\rho=N_r\mu_r$ and the empirical roton effective mass $\mu_r=0.4m_4$,[27] we find for the number of rotons $\rho N_r=1.66\times10^{22}$ per cm^3 at 1.8°K. Thus, the volume percentage of He^3 atoms to rotons is 4.1%, while the viscosity is reduced by 7%; we therefore estimate that the roton-He^3 cross section is 1.7 times that for roton-roton collisions. The semiempirical value for the latter[23] is given as $5\times10^{-15}\ T^{-\frac{1}{2}}$ cm^2; we obtain for the value of the roton-He^3 cross section about 6.3×10^{-15} cm^2. Since the simple ideas proposed for this interaction suggest that the collision cross section should be approximately geometrical, we compare the above empirical value with the projected area of a sphere of liquid containing 7 He^4 atoms. This is 5.8×10^{-15} cm^2.

[26] L. Landau, J. Phys. (U.S.S.R.) **5**, 71 (1941).
[27] R. P. Feynman and M. Cohen, Phys. Rev. **102**, 1189 (1956).

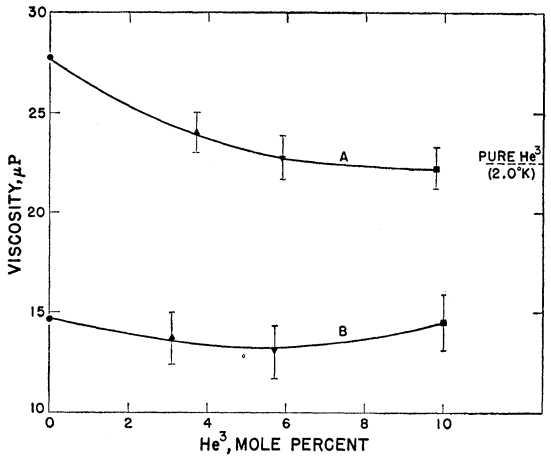

FIG. 10. Dependence of viscosity on He^3 concentration. Curve *A*, viscosities at the lambda temperatures; Curve *B*, viscosities at minima.

In spite of the agreement between these independent values we do not believe that the estimate is dependable to better than an order of magnitude. In particular, the uncertainty in roton effective mass is indicated by the discrepancies between the value $\mu_r=0.4m_4$ which we have used, the earlier estimate $\mu_r=0.77m_4$,[26,27] and $\mu_r=1.7m_4$ which we obtain by a comparison of ρ_n [1] and specific heat[21] at 1.80°K, using $\Delta/k=10.60$°K. Furthermore, the calculated value of the roton-roton cross section depends upon the choice of the roton effective mass.

The over-all dependence of the viscosity on x_3 must be concave upward since η must approach the higher He^3 value at greater concentrations. Although this trend is empirically confirmed, we can make no theoretical estimate of the concentration at which $d\eta/dx_3$ is zero.

Despite the highly speculative character of the arguments and the need for more precision in the measurements, we do appear to find a qualitative correspondence between this simple model and the observed effect of He^3 on the viscosity of He II.

ACKNOWLEDGMENT

We gratefully acknowledge the comments of Professor J. R. Pellam, who originally pointed out the effect of imperfections of a finned rotor upon normal density measurements.